

All-spherical telescope with extremely wide field of view

V. Yu. Terebizh^{1,2*}

¹Crimean Astrophysical Observatory, Nauchny, Crimea 298409

²Institute of Astronomy RAN, Moscow 119017, Russian Federation

February 07, 2016

Abstract

An all-spherical catadioptric telescope with the angular field of view of several tens of degrees in diameter and spherical focal surface is proposed for the monitoring of large sky areas. We provide a few examples of such a system with the apertures up to 800 mm and the field of view 30° and 40° in diameter. The curvature of the focal surface is repaid by high performance of the telescope. In particular, the diameter of a circle, that includes 80% of energy in the polychromatic image of a star, is in the range $1.4'' - 1.9''$ across the field of 30° size and $2.2'' - 2.9''$ for the field of 40° size. Some ways of working with curved focal surfaces are discussed.

1 Introduction

There are two primary modes in surveying of large areas of the sky: 1) we need to cover *sequentially* the area in the reasonable time; 2) the sky area we are interested in should be under *continuous* watching, as is the case when we look for the fast transient objects. To some extent, problems of the first kind can be solved with the help of wide-field telescopes with a flat field of view, such as those discussed by Wilson (1996) and Terebizh (2011). It is easily

*E-mail: valery@terebizh.ru

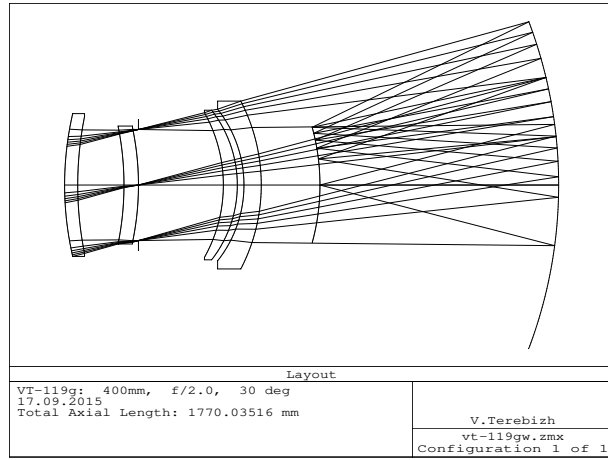


Figure 1: Optical layout of design VT-119g with entrance pupil diameter of 400 mm and a 30° field.

seen that problems of the second kind require too many flat-field telescopes, so it seems that the better way in this case is the creation of a single telescope with an extremely wide angular field, even at a spherical focal surface.

Just this way was chosen in the second half of the last century, when the Baker-Nunn (Henize 1957; Baker 1962), Hawkins and Linfoot (1945), and Maksutov-Sosnina (1950s, unpublished) cameras were put into operation. Their angular field attained 20° – 30°, whereas the shielding of light and curvature of the focal surface were taken into account by application of narrow emulsion tape. The main disadvantages of these cameras were as follows: 1) some lens surfaces were substantially aspheric; 2) the demanding sorts of glass were used in the correctors; 3) nevertheless, the image quality was inadequate. For example, four surfaces of the Baker-Nunn camera were aspheres of 4th and 8th orders, the Schott KzFS2 and SK14 glasses were applied, but the rated image of a point-like source of light was nearly 100 μm (40'') in diameter (Carter et al. 1992). Later modification of the Baker-Nunn camera with aspheric surfaces of the same order but larger aperture provides 1 arc minute resolution in a narrow spectral band (Sasaki et al. 2002).

In view of the above, it was somewhat surprisingly that an *all-spherical system made of simplest types of glass* yet provides nearly diffraction-limited polychromatic images in the field of the order of 30° in diameter (Terebizh

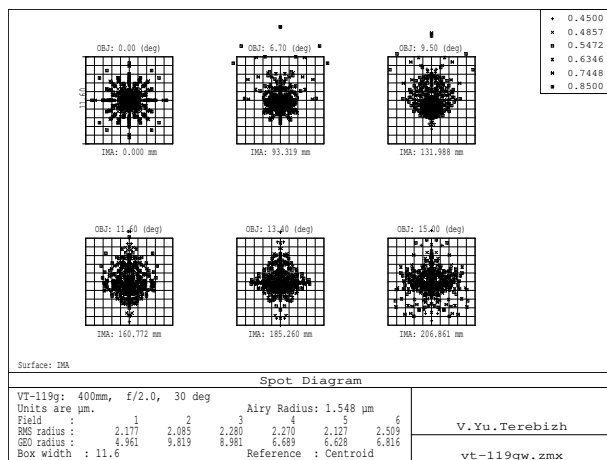


Figure 2: Spot diagram of VT-119g in the polychromatic waveband $0.45 - 0.85 \mu\text{m}$. The field angles are 0° , 6.7° , 9.5° , 11.6° , 13.4° and 15.0° (equal areas). Airy disc diameter is $3.1 \mu\text{m}$, box width is $11.6 \mu\text{m} \simeq 3''$.

2015). A few further examples of such a system are given below¹.

2 All-spherical telescope with a 30° field

An example shown in Fig. 1 has been designed for the aperture 400 mm, effective focal length 800 mm ($f/2.0$), waveband $0.45 - 0.85 \mu\text{m}$ and the 30° field of view. All lenses can be made of the same material; we prefer the fused silica because of its stability and excellent optical properties, in particular, high UV-transparency.

As one can see from Fig. 2, the image quality is nearly constant across the field. More specifically, the D_{80} – diameter of a circle, that includes 80% of energy in the polychromatic image of a star, varies from $5.4 \mu\text{m}$ ($1.4''$) on the optical axis to $7.3 \mu\text{m}$ ($1.9''$) on the edge of the field. The complete description of the system is given in Table 1.

The proposed system proceeds from the two generic versions of the Bernhard Schmidt (1931) camera, that were then developed by A. Bouwers (1941, 1946), D.D. Maksutov (1944), D.G. Hawkins and E.H. Linfoot (1945), C.G.

¹In calculations, we used the *Zemax* optical program (ZEMAX Development Corporation, U.S.A.).

Table 1: VT-119g design with an aperture of 400 mm and 30° field of view. The effective focal length is 800 mm.

Surf. No.	Comments	R_0 (mm)	T (mm)	Glass	D (mm)
1	L1	1141.913	47.0	FS	511.8
2		1241.285	165.714	–	490.1
3	L2	–1060.80	51.871	FS	422.5
4		–997.351	0.0	–	410.1
5	Stop	∞	304.135	–	397.9
6	L3	–530.106	50.0	FS	518.3
7		–436.465	23.871	–	536.0
8	L4	–438.102	62.0	FS	543.4
9		–653.243	1065.44	–	601.2
10	M1	–1656.21	–855.191	Mirror	1169.6
11	Image	–781.790	–	–	413.8

Notes to Table 1:

R_0 – paraxial curvature radius, T – distance to the next surface, D – diameter, FS – fused silica. All surfaces are spheres.

Wynne (1947) and J.G. Baker (1945, 1962)². Our current goal is to get rid completely of aspheric surfaces. This is partly achieved by introduction the modified double meniscus of Wynne (1947), i.e., the first and forth lenses in Fig. 1; the two inner lenses were inserted both to minimize coma and spherochromatic aberration³. The double-meniscus corrector was applied by Baker in his super-Schmidt design, but he placed inside a highly aspheric correction plate such as that introduced by Schmidt. Meanwhile, the only possibility to achieve the true point symmetry about the center of the entrance pupil is to use a purely spherical optics.

The point symmetry both of the fundamental form of a wide-field telescope consisting of an idle stop at the center of curvature of a spherical mirror (J. Petzval, H. Vogel, K. Strehl) and the basic Schmidt’s model is closely re-

²See Wachmann (1955); Busch, Ceragioli and Stephani (2013) for historical roots, Wilson (1996); Rutten and Venrooij (1999); Schroeder (2000) and Terebizh (2011) for specifications and discussion.

³The system with only three lenses provides noticeably worse images than the discussed one, while the increasing the number of lenses slightly improves images, but seems too massive.

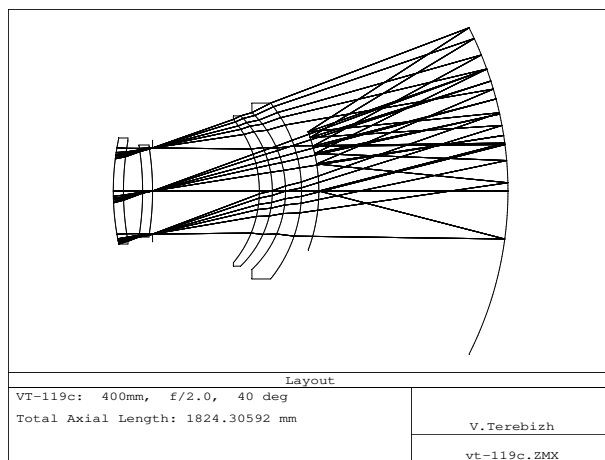


Figure 3: Optical layout of design VT-119c with entrance pupil diameter of 400 mm and a 40° field.

lated to the fact that the entrance pupil coincides with the aperture stop. To a good approximation, the same is also true for our design.

Another its important feature is that the optical power of the system is provided by the mirror, while the four-lens corrector working at $f/44$ is nearly afocal. Just that should be the case to prevent the chromaticity at reducing spherical aberration inherent to the spherical mirror. The resulting width of the chromatic focal shift curve is $10.5 \mu\text{m}$, whereas it should be less than $\sim 9 \mu\text{m}$ for an ideal, diffraction-limited system. Besides, a small optical power of the lens corrector greatly contributes – along with the spherical shape of surfaces – to the mitigation of general tolerances.

As regards losses of light, a strip-like detector of size $30^\circ \times 5^\circ$ ($39 \text{ cm} \times 6.5 \text{ cm}$) shields less than 7% of flux.

Obviously, individual light detectors may be arranged freely, both continuously and discretely. An optimum way is to arrange them in accordance with the shape of the observed sky area.

3 All-spherical telescope with a 40° field

To illustrate the capabilities of the optical layout under discussion, we give in Fig. 3 and Table 2 an example of a 40° -design VT-119c, which spherical lenses are made of fused silica and simplest glasses Schott N-F2 and N-BK7.

Table 2: VT-119c design with an aperture of 400 mm and a 40° field. The effective focal length is 800 mm.

Surf. No.	Comments	R_0 (mm)	T (mm)	Glass	D (mm)
1	L1	1190.292	47.000	FS	490.4
2		1305.352	88.531	–	463.9
3	L2	–1326.54	46.000	N-F2	425.5
4		–1300.49	0.000	–	410.8
5	Stop	∞	493.552	–	398.5
6	L3	–516.800	60.000	FS	662.2
7		–484.196	60.969	–	694.6
8	L4	–501.003	74.000	N-BK7	725.2
9		–649.809	954.254	–	813.0
10	M1	–1671.01	–874.182	Mirror	1509.0
11	Image	–777.519	–	–	546.7

Notes to Table 2:

Designations are the same as in Table 1. The glasses N-F2 and N-BK7 are from the Schott sample. All surfaces are spheres.

A similar system that uses only fused silica provides just a little inferior image quality, but is more expensive.

The effective focal length of VT-119c is still equal to 800 mm, the design waveband remained 0.45 – 0.85 μm . As before, the image quality is nearly fixed across the field: the diameter D_{80} of a star image varies in the range 8.5 – 11.1 μm (2.2" – 2.9"). The width of the chromatic curve, 27.8 μm , is not far from that for the diffraction-limited system, 10.2 μm .

4 Survey speed and limiting magnitude

When working with wide-field telescopes, most important characteristics are the survey speed S (degree²/second) and limiting magnitude m_{lim} given the exposure time T . Let us consider in this context the VT-119g design with the rectangular field of view of, say, 30° × 5°, giving the observed sky area $\Omega = 150 \text{ deg}^2$ (the diameter of the equivalent circular field $2w_e \simeq 13.8^\circ$). It was assumed that the noise obeys the Poisson distribution. Assuming also that the telescope image quality $D_{80} = 1.7''$, its transparency is 0.85, the

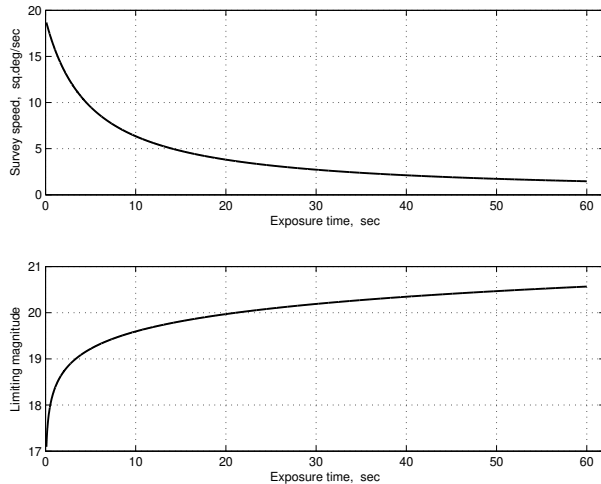


Figure 4: Survey speed S (deg^2/sec , upper curve) and limiting magnitude m_{lim} as the functions of the exposure time (sec) for the VT-119g design.

fraction of unvignetted rays $U = 0.90$, the quantum efficiency of detector is 0.85 counts/photon, pixel size is $9\mu\text{m}$, the atmosphere seeing $\beta_{atm} = 1.5''$, the sky background is $20.0^m/\text{arcsec}^2$, the optical thickness of the atmosphere in zenith is 0.30, the object zenith angle is 40° , the dead time⁴ is 5 sec, and the threshold signal-to-noise ratio $S/N = 8$, we come to results shown in Fig. 4. Our estimates of limiting magnitude were performed by standard methods, they are in a good agreement with those according to the SIGNAL package created by the team of the Isaac Newton Group of Telescopes (<http://catsserver.ing.iac.es/signal/>). The survey speed is simply the field area divided by the sum of the exposure time and dead time.

Evidently, the large field of view entails high survey speed of the system. It is enough to say that at the exposure time 4 sec the survey speed of $11\text{ deg}^2/\text{sec}$ is attained, so the objects brighter than $\sim 19^m$ can be registered in the sky area of 10^4 deg^2 in 15 minutes.

As regards limiting magnitude, it is difficult to expect its high value for a telescope of relatively small size. We see that for short exposures, which are specific to fast transients, the objects not fainter than about 19.5^m are attainable. The limit is increased to 20^m at the exposure time of 20 sec. To reach more faint sources, the proposed optical system can be scaled up,

⁴The ‘dead time’ is the sum of read-out and telescope redirection time spans.

the more that the image quality is very weakly dependent on the size of the system (see the next section).

It seems quite evident that the significant survey efficiency, including both the deep limit and high speed, can be achieved by creating a hierarchical system, consisting of different types of telescopes.

Let us also estimate the *sky survey rate* Γ , that was defined in the review of Terebizh (2011) by equation (A2). It is simply the product of the observed sky area Ω (degree²) and effective aperture area of the telescope $A = \pi D_e^2/4$ (meter²), divided by the squared image quality Δ (arc seconds):

$$\Gamma \equiv \Omega \cdot A/\Delta^2 \quad \textit{Herschels}, \quad (1)$$

where, by definition, the measurement unit is *Herschel* $\equiv 1 \text{ m}^2 \text{ deg}^2 / \text{arcsec}^2$ (shortly denoted by *H*). For the fraction of unvignetted rays $U = 0.90$ and the delivered image quality $\Delta = 3.4''$ we obtain the effective aperture diameter $D_e \simeq 0.38$ m and the survey rate $\Gamma \simeq 1.5 H$. Even with such a small part of the available field, this is a significant value.

As was mentioned, detectors may be positioned arbitrarily in the field of view. In this connection Tonry (2015) noted, that some optimal summary area of detectors to maximize Γ should exist, because by expanding the operating area we increase Ω , but reduce the effective aperture of the telescope D_e due to larger obscuration. Our approximate analytical calculations show that this is the case; an accurate assessment can be found for each specific task.

5 Scaling of the system

Scaling both up and down leads to attractive systems; we confine ourselves to the first option.

Model VT-119f (Table 3) with the aperture 800 mm in diameter is a slightly optimized doubling of the design VT-119g at the same angular field size. As before, all lenses are spherical and made of fused silica. It turned out that the image quality of both systems, the original and scaled one, is substantially the same in the angular measure, $D_{80} \simeq 1.7''$. This means, in particular, that for the equal exposure times system VT-119f provides about one magnitude fainter objects, than VT-119g. (The doubling of diameter gives only 0.75^m , but we get an additional gain due to increased focal length.)

Table 3: VT-119f design with an aperture of 800 mm and 30° field of view. The effective focal length is 1520 mm ($f/1.90$).

Surf. No.	Com-ments	R_0 (mm)	T (mm)	Glass	D (mm)
1	L1	2411.655	94.000	FS	1035.1
2		2670.891	351.049	–	992.5
3	L2	–1955.47	104.000	FS	846.7
4		–1854.17	0.000	–	822.9
5	Stop	∞	611.829	–	796.4
6	L3	–1005.61	100.000	FS	1034.0
7		–854.950	54.835	–	1072.4
8	L4	–861.958	124.000	FS	1090.1
9		–1251.91	1988.336	–	1206.7
10	M1	–3151.84	–1629.20	Mirror	2273.9
11	Image	–1484.81	–	–	786.2

Notes to Table 3:

Designations are the same as in Table 1. All surfaces are spheres.

Since the system under consideration can be essentially scaled up at maintaining angular resolution over the whole field, one can get a theoretical design of even larger aperture. Unfortunately, not optics by itself, but practical limitations on a lens size put the limit on further scaling. In particular, the diameter of the last lens in the system VT-119f is about 1.2 m, which is already not far from the size reached by the modern technology based on the use of glass. Because of soft tolerances, some plastic materials may be promising for the lenses. For example, replacement of fused silica in the system VT-119f with acrylic reduces the weight of the lens corrector twice at the same image quality and transparency in a wide spectral range. Perhaps, further research will produce the more stable lenses made of plastic materials, especially of a simple spherical shape.

Another way, which is worth studying now, is to use the proposed design as the core of some light-gathering system of larger size.

6 Concluding remarks

The curvature of the focal surface is as natural for wide-field telescopes, as for the human eye. The key step at the transition from conventional telescopes to really wide-field systems is changing the type of symmetry of an optical system. As noted by G.H. Smith (1998) concerning the Schmidt camera,

There is now point symmetry about the center of the stop (and the center of curvature of the mirror), rather than rotational symmetry about an axis.

However, it must be admitted that the point symmetry is insufficiently perfect as long as aspheric surfaces are used, and only application of the all-spherical optics makes it strict except inevitable vignetting of the aperture stop. Just this feature allowed to expand radically the field of view. It can be shown that the proposed here all-spherical system provides the high quality images with the field size of more than 50° .

Perhaps, the Cassegrainian versions of the system are possible only for not too wide angular field, say, not larger than 10° . Behind this approximate boundary, it is difficult to account for the curvature of the focal surface.

Of course, large curved light detectors, the production of which has just begun, will be used in future. This field is developing rapidly. The principal issues and real examples are discussed by Iwert and Delabre (2010), Iwert et al. (2012); the first paper includes a photograph of curved detector with size of $60 \text{ mm} \times 60 \text{ mm}$ and curvature radius 500 mm. There are also working devices of this type. In particular, curved detector has been implemented in the DARPA 3.5 m Space Surveillance Telescope (Blake et al. 2013).

Besides, one need to keep in mind the long-known technology based on a plurality of delicate waveguides with a curved in aggregate input faced to the focal surface.

The method of working with the spherical focal surface applicable currently is the using of small flat detectors each of which is equipped with a flattening lens. This way has been implemented, e.g., in the *Kepler* space telescope that has the 95 cm aperture and the equivalent field diameter of 11.6° . Its detector consists of 21 pairs of ordinary $59 \text{ mm} \times 28 \text{ mm}$ CCDs covered by sapphire field-flattening lenses. As to the VT-119g design, the curvature radius of its focal surface is 782 mm, so with a small flat detector of size, say, 25 mm the edge images are blurred up to 50 microns. Our

preliminary consideration shows that the image quality can be improved considerably even by a single lenslet made of fused silica, and is fully recovered by the doublet of the same material. The problem becomes much simpler for larger telescopes similar to VT-119f.

It seems likely that further research will expand the scope of the proposed optical layout. In particular, applications in the spectroscopy, physics of cosmic rays, geophysics and tomography are especially promising.

Acknowledgments

I thank M.R. Ackermann (University of New Mexico, U.S.A.), M. Boer (Recherche CNRS ARTEMIS, France), R. Ceragioli (University of Arizona, U.S.A.), Yu.A. Petrunin (Telescope Engineering Company, U.S.A.), W. Stephani (Hamburg University, Germany) and J.L. Tonry (Institute for Astronomy, University of Hawaii, U.S.A.) for creative discussions. Referee proposals were useful.

References

- [1] Baker, J.G. 1945, U.S. Patent 2,458,132
- [2] Baker, J.G. 1962, U.S. Patent 3,022,708
- [3] Blake T., Pearce E., Gregory J.A., Smith A., et al., 2013, AMOS Technical Conference, 57
- [4] Bouwers, A, 1946, Achievements in Optics, Elsevier, Amsterdam, 25
- [5] Busch, W., Ceragioli, R.C., Stephani, W. 2013, Journal of Astronomical History and Heritage 16(2), 107
- [6] Carter, B.D., Ashley, M.C.B., Sun, Y-S., Storey, J.W.V. 1992, PASA 10, 74
- [7] Hawkins, D.G., Linfoot, E.H. 1945, MNRAS 105, 334
- [8] Henize, K.G. 1957, Sky and Telescope 16, 108
- [9] Iwert, O., Delabre, B., 2010, Proc. SPIE 7742-27

- [10] Iwert, O., Ouelette, D., Lesser M., Delabre, B., 2012, Proc. SPIE 8453-68
- [11] Maksutov, D.D. 1944, J. Opt. Soc. Am. 34, 270
- [12] Rutten, H.G.J., van Venrooij, M.A.M. 1999, Telescope Optics, Willmann-Bell, Ch. 8
- [13] Sasaki, M., Kusaka, A., Asaoka, Y. 2002, arXiv:astro-ph/0203348v2
- [14] Schmidt, B. 1931, Centr. Ztg. f. Opt. u. Mech., 52, 25
- [15] Schroeder, D.J. 2000, Astronomical optics, Academic Press, Ch. 7
- [16] Smith, G.H. 1998, Practical Computer-Aided Lens Design, Willmann-Bell, Richmond, p. 380
- [17] Terebizh, V.Yu. 2011. Astron. Nachr. / AN, 332, 714
- [18] Terebizh, V.Yu. 2015, arXiv:1507.07110v1 [astro-ph.IM] 25 Jul 2015
- [19] Tonry, J.L. 2015, Private communication
- [20] Wachmann, A.A. 1955, Sky and Telescope 15, No. 1, 4
- [21] Wilson, R.N. 1996, Reflective Telescope Optics, Springer, V. I, Section 3.6
- [22] Wynne, C.G. 1947, MNRAS 107, 356